Thermal Deformation of Very Slender Triangular Rollable and Collapsible Booms

Olive R. Stohlman[1]
NASA Langley Research Center, Hampton, VA, 23666, USA

Erik R. Loper[2]
NASA Marshall Space Flight Center, Huntsville, AL, 35812, USA

Metallic triangular rollable and collapsible (TRAC) booms have deployed two Cubesat-based solar sails in low Earth orbit, making TRAC booms the most popular solar sail deployment method in practice. This paper presents some concerns and solutions surrounding the behavior of these booms in the space thermal environment. A 3.5-cm-tall, 4-meter-long TRAC boom of Elgiloy cobalt alloy, when exposed to direct sunlight in a 1 AU deep space environment, has a predicted tip motion of as much as 0.5 meters. Such large thermal deflections could generate unacceptable distortions in the shape of a supported solar sail, making attitude control of the solar sail spacecraft difficult or impossible. As a possible means of mitigating this issue, the thermal distortion behaviors of three alternative material TRAC booms are investigated and compared with the uncoated Elgiloy baseline boom. A tenfold decrease in induced curvature is shown to be possible relative to the baseline boom. Potential thermal distortions of the LightSail-A solar sail TRAC booms are also examined and compared, although inconclusively, with available on-orbit camera imagery.

I. Introduction

Triangular rollable and collapsible (TRAC) booms, originally developed at the US Air Force Research Laboratory (AFRL), are a class of tape-spring booms characterized by a triangular cross-section [1]. This cross-section can be seen in Figure 1, and can be flattened and rolled like a carpenter's tape for storage, as depicted in Figure 1(a). TRAC booms have been produced in metallic and composite materials [2]. NASA's Nanosail-D2 [3] and the Planetary Society's LightSail-A [4] solar sails were deployed by TRAC booms, and the upcoming Planetary Society LightSail-B will also be deployed by TRAC booms. No other rigid deployable boom has been used to deploy a solar sail in space.

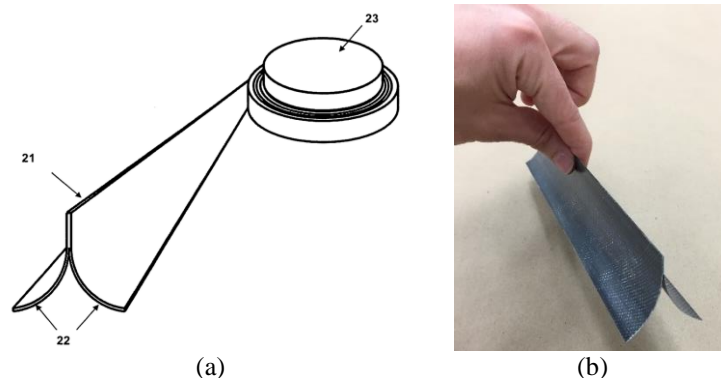(a)   (b)

Figure 1: The TRAC boom concept and cross-section. The fundamental shape is seen in this picture (a) from the patent [1]. It can be realized in a variety of materials and sizes; (b) shows a composite TRAC boom section that can be flattened to a cross-sectional height of 45 mm.

---

[1] Research Aerospace Engineer, Structural Dynamics Branch, AIAA Member.
[2] Aerospace Engineer, Thermal and Mechanical Analysis Branch.

American Institute of Aeronautics and Astronautics

TRAC booms are also part of the baseline design for the Near Earth Asteroid (NEA) Scout [5] Cubesat; the content of this paper was developed in the context of the NEA Scout and Lunar Flashlight [6] programs. Figure 2 shows the 6U NEA Scout Cubesat with its reflective solar sail deployed to a full size of approximately 10 by 10 meters. The 6U Cubesat satellite bus and its deployable solar panels are visible at the center of the much larger sail, whose systems occupy approximately half of the satellite volume when stowed.

As TRAC-deployed Cubesat solar sails get larger and larger, new structural effects become increasingly significant. This paper addresses the thermal deformation of TRAC booms in a space environment, a geometric distortion of the boom that would be quite significant in a 10-meter-class solar sail. While these deployable sails typically have low precision requirements, gross boom distortions of tens of centimeters can move the center of pressure and reduce the booms' structural performance. It is possible to ameliorate the thermal distortion in a number of ways: arranging the sail membrane to shade the booms from direct sunlight and using composite booms with a low axial coefficient of thermal expansion (CTE) are promising approaches.
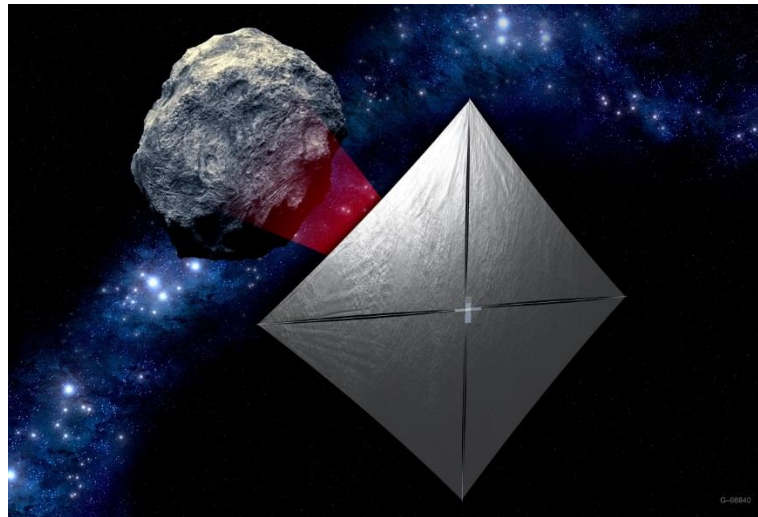

Figure 2: Artist's illustration of the NEA Scout mission concept.

The purpose of this investigation is to understand the magnitude of the thermal deformation of this popular deployable structure. Thermal-mechanical finite element analysis of an uncoated metallic TRAC boom at a range of sun angles is presented as the first result, and shows significant deformation of the booms. This finding motivates three further questions: Can the thermal deformation be reduced with a simple change of materials? Does this boom deformation have an effect on the overall shape of a solar sail, or does the sail membrane enforce the sail shape? Can we demonstrate the real-world impact of this analytically supported effect in past or upcoming missions? These questions are addressed with simulations of boom compression in isolation, simulations of booms in a basic solar sail structure, and the projection of a set of simulated deformed booms onto existing images of a solar sail in space.

The remainder of this paper is organized as follows: A brief background on Cubesat-based solar sails and thermal deformations of gossamer structures is presented in the remainder of the introduction; the thermal and structural models are presented in Section II; results of the modeling are presented in Section III. Section IV is a limited analysis of the imaging data from the Planetary Society's recent LightSail-A mission. Section V concludes with remarks on design and analysis.

A. Deployable Tape-Spring Booms

Deployable tape-spring booms make excellent use of volume. They can be stowed with very little wasted space, and the parasitic volume percentage continues to decrease with boom length. There is a natural attraction between Cubesats, which are subject to strict volume constraints, and tape-spring booms. A partial listing of recent projects using deployable tape spring booms includes NASA's Nanosail-D [3], the Planetary Society's LightSail [7], the European Union's Deorbitsail [8], the University of Surrey's multiple sail projects [9], the Deutsches Zentrum für Luft und Raumfahrt (DLR) Gossamer project [10], and ClydeSpace's AEOLDOS off-the-shelf deorbiting system [11] all use or used booms that flatten and coil.

American Institute of Aeronautics and Astronautics

B. The Space Thermal Environment and Large Structures

Extreme temperatures are a common feature in space missions. Gossamer structures, in particular, may experience thermal deformations that are large enough to be clearly visible to the naked eye, but most are known purely as analysis results.

Blandino [12] has presented a coupled thermal-structural analysis of Storable Tubular Extendable Member (STEM) booms, a type of rollable boom with a slit circular cross-section. For large structures, geometry changes may be large enough that a single thermal analysis is not acceptable, and coupling (or slower sequential iteration) must be introduced to capture the simultaneous changes in geometry and temperature distribution. The DLR closed-section lenticular boom has also undergone thermal analysis [10]; both STEM and closed-section lenticular booms benefit from the low coefficient of thermal expansion of their composite materials in these designs.

A study of the Gravity and Extreme Magnetism Small Explorer (GEMS) telescope boom [13] predicted advantages to shading the structure with a Kapton "sock;" in the case of this high-precision truss boom, the shape distortion could be reduced by an order of magnitude by protecting the structure from direct sunlight.

II. Modeling

Because the booms are very slender, visualizations that show the entire sail (e.g., Figure 3(a)) are not useful in understanding boom behaviors like twisting. Many of the visualizations in this paper show an extremely foreshortened view down the length of the boom, as in Figure 3(c).
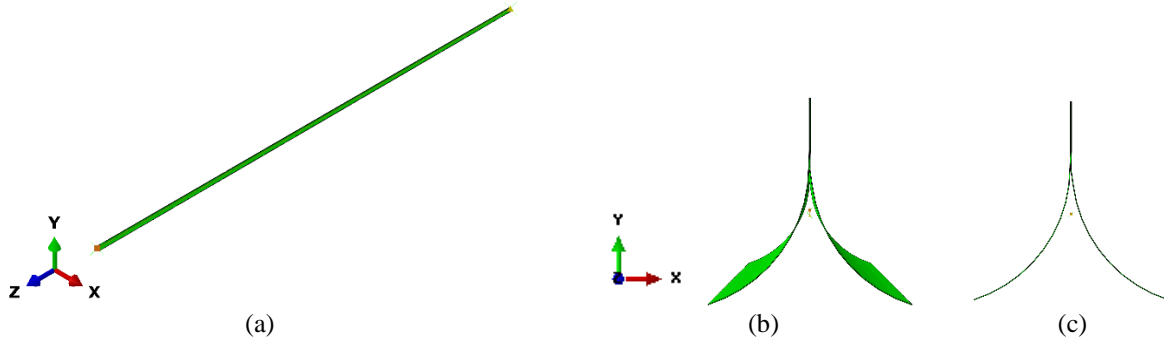

(a)   (b)   (c)

Figure 3: Three views of the "floating" boom model (4 meter length). The axial direction of the boom is Z. Overhead view (a), perspective view from end (b) and parallel projection from end (c).

A sequential thermal-stress analysis approach was used in this investigation. The stages of analysis were as follows:
1. Static stress analysis of the sail system, establishing the root condition and preloading of the sail
2. Steady-state thermal radiative analysis of the deformed sail system in a mission-relevant space environment
3. Static stress analysis of the sail system, resumed from the preloaded condition, with the temperature field applied as a boundary condition

There was no form of heat transfer analysis in the stress analysis stages, nor any stress analysis performed in the thermal analysis stage. Where stage 3 indicates a very large deformation (e.g., 15 degrees of boom twist), the new deformed shape can be returned to stage 2 and the temperature field reevaluated. Results presented here were not iterated in this way. As demonstrated by Blandino [12], more closely coupled analysis is possible; sequential coupling was preferred for faster setup in this analysis.

Two structural models have been used in evaluating the significance of thermal deformation. The first is a simple "floating boom" model (Figure 3), where the boom is analyzed alone, without any representation of the sail. The second is the more complex boom-and-membrane model (Figure 4), where a realistic root condition is added to the model and the interactions with a highly simplified membrane are considered. The floating boom uses a 4-meter boom and the boom-and-membrane model uses 7.3-meter booms.
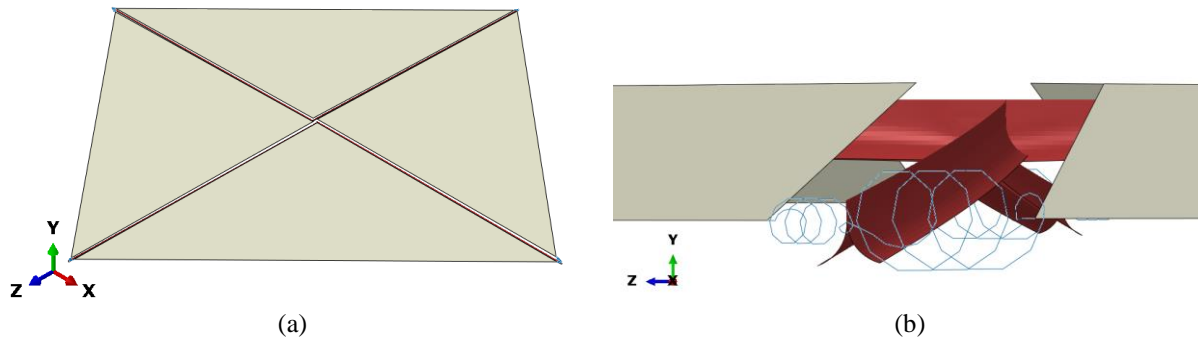
American Institute of Aeronautics and Astronautics

Figure 4: Perspective view of the boom-and-membrane quadrant model (approx. 10 meter edge length). Sail quadrants are grey; TRAC booms are red; spring elements are blue. (a) View of sun side (b) View down length of boom (perspective)

The floating boom model is much simpler, so it is used as the most direct comparison for coating and material performance. The boom-and-membrane model is, however, the only way to evaluate mission-critical effects and the sail's compliance with requirements.

The modeled TRAC boom flattens to a height of 3.5 cm. Two 7.3-meter-long Elgiloy booms can be co-coiled and stowed within a 10-cm-by-10-cm Cubesat footprint.

A. Materials

Three materials are considered here, and represent a range of responses to the problem of thermal expansion: uncoated Elgiloy is considered as a baseline; the relatively practical coating of vapor-deposited aluminum (VDAL) on Elgiloy as an alternative in a mission where the Elgiloy design is preferred; and two composite alternatives, demonstrating the improvements in thermal behavior in combination with the structural compromises of a composite option. In many cases, composites are structurally superior in elastically stowed booms. However, for very thin shells, Elgiloy is a stiffer material and composite options are limited. In this study, the composite alternatives bracket the thickness of the Elgiloy.

Composite A is a one-ply 0/90° plain weave and somewhat thinner than the Elgiloy shell. Composite B is a two-ply laminate with a 0/90° plain weave ply and a 0° unidirectional ply; this is 40% thicker than the Elgiloy shell. Material properties are summarized in Table 1 and Table 2. Composite properties are based on theoretical calculations, not laboratory measurements.

Table 1: Structural properties of candidate materials

	Young's modulus (axial) (GPa)	Coefficient of thermal expansion (axial) (µm/m/K)	Thickness (mm)	Linear density (g/m)
Elgiloy	200	12.7	0.10	60
Carbon fiber composite A (thin)	80	1.3	0.09	10
Carbon fiber composite B (thick)	114	0.8	0.14	16

Table 2: Thermal properties of candidate materials

	Thermal Conductivity (transverse) (W/m·K)	Density (kg/m³)	Emissivity	Solar absorptivity
Elgiloy	12.5	8300	0.107	0.43
Vapor deposited aluminum coating	--	--	0.08 [14]	0.02
Carbon fiber composite A (thin)	4.3	1580	0.75 [15]	0.92
Carbon fiber composite B (thick)	3.3	1580	0.75	0.92

B. Thermal Modeling

The thermal environment was created using the Thermal Desktop orbit tool. The environment for the floating boom cases places a single boom at 1 Astronomical Unit (AU) from the sun. For the boom-and-membrane model, a position near the southern lunar pole at an altitude of 20 km was used to create the thermal environment. The moon was modeled with a planet shine of 122.8 °C for the hot side and -233.15 °C for the dark side. Albedo and solar flux were modeled using an albedo of 0.1, and a solar flux of 1354 W/m². The orientation of the satellite and the orbit were defined with two vectors, listed in Table 3.

Table 3: Solar and Planet vector used to define the orientation and location of the lunar flashlight satellite during the science portion of the Lunar Flashlight mission. The coordinate frame is the same as in Figure 4.

Vector	X	Y	Z
Solar	0.0000	0.7071	-0.7071
Planet	0.0000	-0.6309	-0.7759

The boom was modeled using Thermal Desktop plate elements. The fused web thickness was 0.204 mm and the legs of the boom were modeled with a thickness of 0.102 mm. The TRAC booms were modeled with the material properties of Elgiloy and a range of optical properties describing different coatings, including the uncoated option of heat-treated Elgiloy; the optical properties were measured at Marshall Space Flight Center. Some of the material and optical properties used in the model are listed in Table 2.

C. Structural Modeling

All structural modeling was performed using Abaqus/Standard [16]. For the floating boom case, a 4-meter boom was modeled. Each boom comprises 28000 S4 shell elements. The nodes of the root cross-section are constrained in the three translational degrees of freedom and the nodes of the tip cross-section are constrained as a rigid body. To evaluate stiffness in compression, the boom was loaded by shortening a connector element between the root and tip centroid. These centroid nodes are rigidly fixed to the root and tip cross-sections.

The unloaded, thermally distorted shape of the floating boom model can be compared with theory by assuming linear distribution of temperature across the cross section. This will induce a constant curvature in the boom. The radius of curvature can be estimated by the following equation:

$$r_{linear} = \frac{h}{\alpha \Delta T}$$

for a boom of height h, coefficient of thermal expansion α, and temperature differential ΔT. Because of the irregular shape of the TRAC cross-section and the nonlinear temperature distribution in the cross-section, this is at most a very approximate estimate of the radius of curvature, but it is useful as an order-of-magnitude estimate. Another possible simplification of the problem assumes a step distribution of temperature, with half of the cross-section at a low temperature and half at a high temperature; this step distribution gives a value of $r_{step} = 2/3 \cdot r_{linear}$. These two values are observed to bound the finite element analysis (FEA) results presented here.

American Institute of Aeronautics and Astronautics

All materials are considered to be elastic, and all material properties are taken as constant with respect to temperature, with the exception of the thermal expansion coefficient of Elgiloy, which is represented as temperature-dependent. Composites are modeled as orthotropic.

In the boom-and-membrane models, each boom comprises 28000 S4 shell elements, with greater element density near the root and tip, as shown in Figure 5. Each membrane quadrant is modeled as a single M3D3 element and the Abaqus *NO COMPRESSION material option is activated.
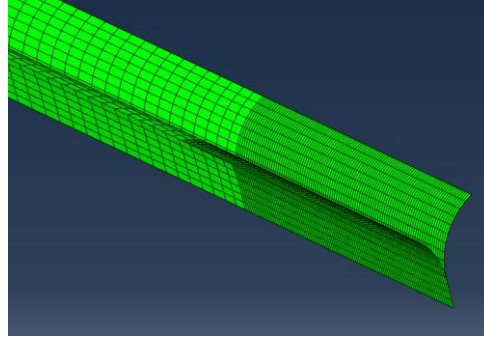
Figure 5: TRAC boom tip with mesh.

In the boom-and-membrane model, the TRAC boom tips are connected to the sail membrane corners by SPRINGA elements with a high rigidity, and at the center of the spacecraft with a constant force spring at 1 N tension. The physical boundary condition on the system is set at the boom root, where a row of nodes on each boom is held in a position that mimics the designed root condition (Figure 6). Stresses from this boundary condition were, in every analysis case, an order of magnitude below the yield stress of the material.

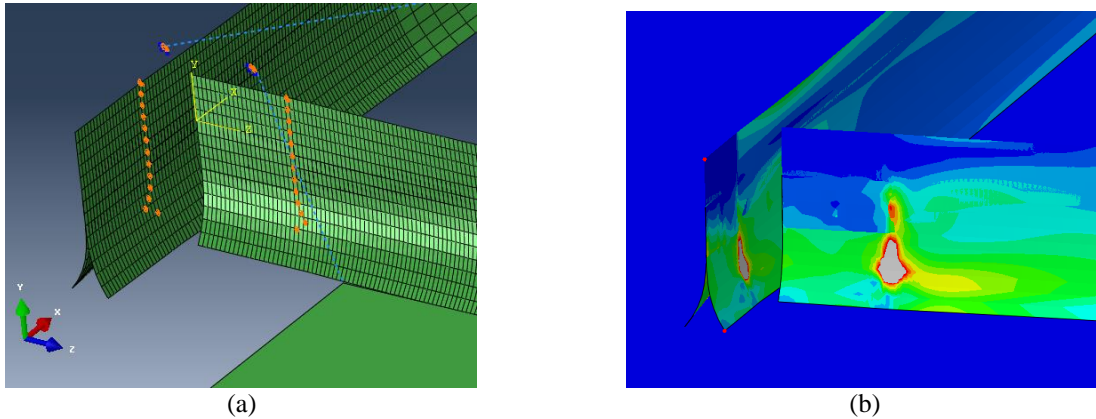(a)   (b)

Figure 6: The boom root condition (a) and associated distribution of von Mises stresses (b). The boom root shape is imported from a previous analysis of the root condition as initially strain-free.

The presence of the membrane synchronizes the motion of the four boom tips, weakly restricting in-plane motion of the booms to a coordinated "windmill" motion.

III. Results

A. Comparison of Different Boom Orientations

Figure 7 illustrates the significant curvature that can be induced in bare Elgiloy TRAC booms when the single floating boom model is subjected to a range of sun angles. As the boom root is rotated through 180° about its long axis, the tip moves towards and away from the sun in a complex pattern. A boom with a simple circular cross-section would always curve away from the sun under these conditions.

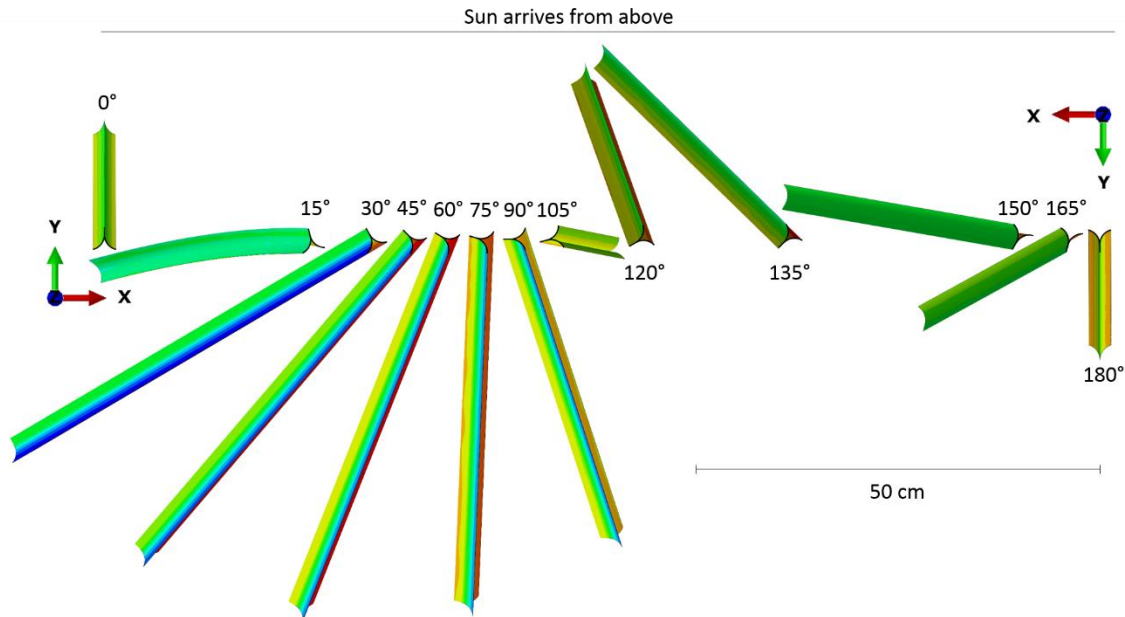American Institute of Aeronautics and Astronautics

Figure 7: The variation in boom deformation with sun angle. As the 4-meter boom spins at the root through 180 degrees about its Z axis, its tip moves towards and away from the sun. The root is held in a cantilevered condition without tilt about the X or Y axes, and a straight boom would appear as in Figure 3(c). View is a parallel projection, viewed from the root as in Figure 3(c); deformations are shown at 1:1 scale.

For the material comparisons, the 45° sun angle is always considered. This angle produces particularly extreme curvature, with the tip rotated by about 15°. The thermal results have not been reevaluated for the distorted boom shapes, and the tilt of the boom tip relative to the sun would produce modestly less curvature far from the root. This is an extreme result for a simple structure, and the dimensions and materials of this model are taken from the same TRAC boom design as the Planetary Society's LightSail-A booms; it is not an improbable or edge case of boom behavior.

B. Comparison of Different Materials

A change in materials affects three outcomes of the analysis: first, the temperature distribution changes according to the thermal properties; secondly, the coefficient of thermal expansion will determine the distorted shape that occurs in response to the temperature distribution; and finally, the new shape and material properties change the structural properties of the boom as a whole.

The performance of the candidate materials was evaluated using the floating boom model. Figure 8 shows the temperature distributions in geometrically identical booms of the two carbon fiber candidate materials, the original uncoated Elgiloy, and Elgiloy with a vapor-deposited aluminum coating. Figure 9 and Figure 10 show the full length of the booms. The induced radius of curvature and the temperature gradient within the cross section are summarized in Table 4. A vapor-deposited aluminum coating on Elgiloy produces the smallest temperature gradient. Because the carbon fiber composites have high absorptivity and emissivity and low conductivity, they experience more extreme temperature gradients than uncoated Elgiloy.
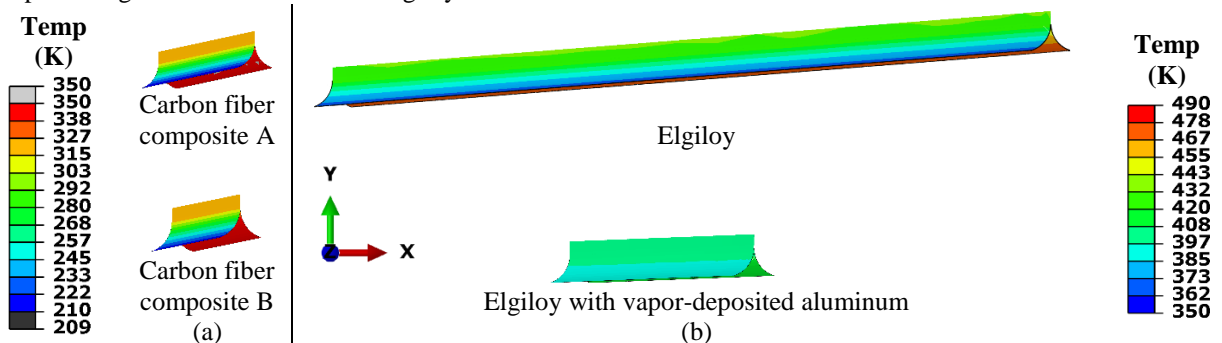
Figure 8: Temperature distributions and tip displacement of four different candidate materials in 45° direct sunlight at 1 AU. View is a parallel projection of the 4-meter booms, viewed from the root.
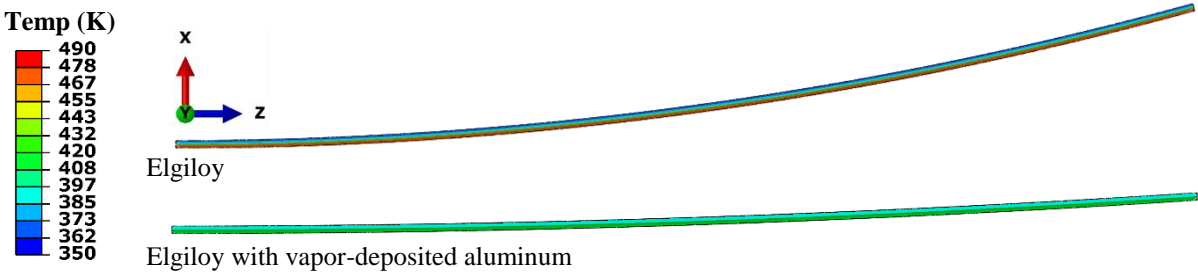

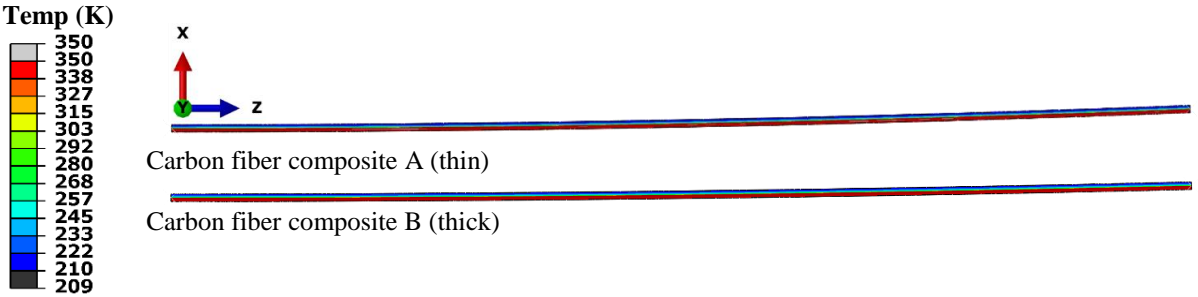*Figure 9: Elgiloy boom thermal distortion, full boom view*

Figure 10: Carbon fiber composite booms thermal distortion, full boom view.

Despite temperature gradients of over 100 K, the carbon fiber composites experience less boom curvature than Elgiloy, because of their low coefficients of thermal expansion. The temperature gradient is more than five times as extreme in composite A as in VDAL-coated Elgiloy, but Elgiloy's coefficient of thermal expansion is nearly ten times higher. The radius of curvature determined by finite element analysis is consistent with theoretical predictions for the modeled temperature gradient in every case.

Table 4: Geometric changes due to thermal distortion (no mechanical load)

	Tip-to-root length change due to thermal deformation (expansion and curvature)	Radius of curvature (FEA)	Radius of curvature range (theory)	Difference between minimum and maximum temperatures within cross section
Elgiloy	-5.3 mm	16 m	14-21 m	103 K
Elgiloy with vapor-deposited aluminum coating	+4.7 mm	62 m	57-85 m	26 K
Carbon fiber composite A (thin)	+1.1 mm	104 m	100-149 m	141 K
Carbon fiber composite B (thick)	-0.1 mm	172 m	166-249 m	135 K

While the carbon fiber composite booms experience relatively little thermal distortion, the material is less stiff than Elgiloy. It may be important to their structural application to provide a certain structural stiffness. The simple case of tip-to-tip compression is illustrative: Figure 11 shows the stiffness in compression of initially straight TRAC booms of uniform temperature. The stiffness of a straight TRAC boom is determined by the material stiffness in the axial direction, up to a level of deformation where local buckling and global bending affect the stiffness. Elgiloy is

American Institute of Aeronautics and Astronautics

stiffer than either carbon fiber composite option considered here, and the Elgiloy booms also have a higher predicted maximum load than either carbon fiber composite.
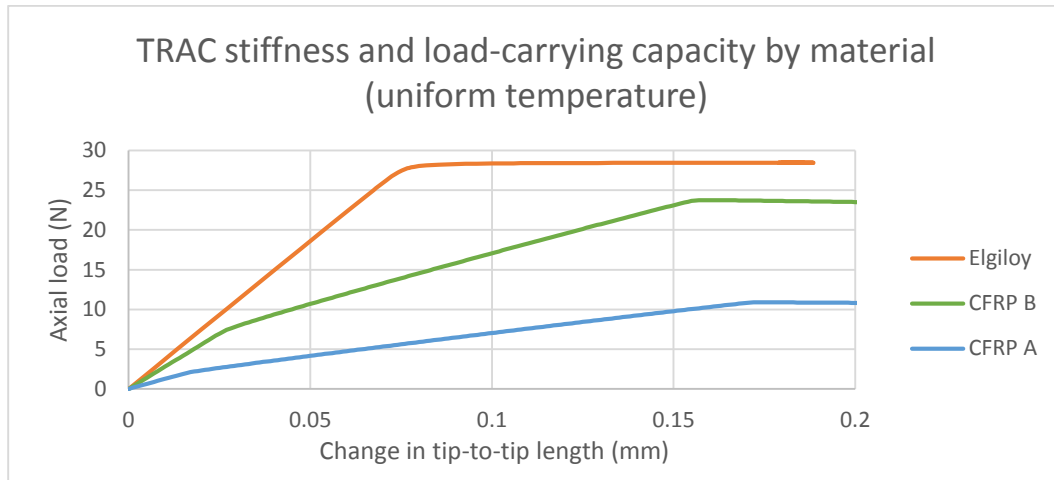

Figure 11: Load-displacement relationships for thermally uniform 4-meter booms of different candidate materials. Loading is in tip-to-root compression.

Regardless of material, all TRAC booms exposed to direct sunlight in the space environment experience significant change in curvature. The stiffness in tip-to-tip loading is now determined by their bending stiffness and the radius of curvature of the thermally distorted boom. This lowers the boom stiffness. In Figure 12, it is evident that every thermally deformed boom is less stiff (at zero load) than every straight boom. The evolution of the boom stiffness with increasing load is shown in Figure 13, and the stiffness results are summarized in Table 5. While Elgiloy initially has the best structural properties, it must be coated to be competitive with even the comparatively flimsy single-ply carbon fiber composite A. The trade between thermal deformation and structural performance is not simple, particularly where thick composites are excluded by a volume-limited design space.
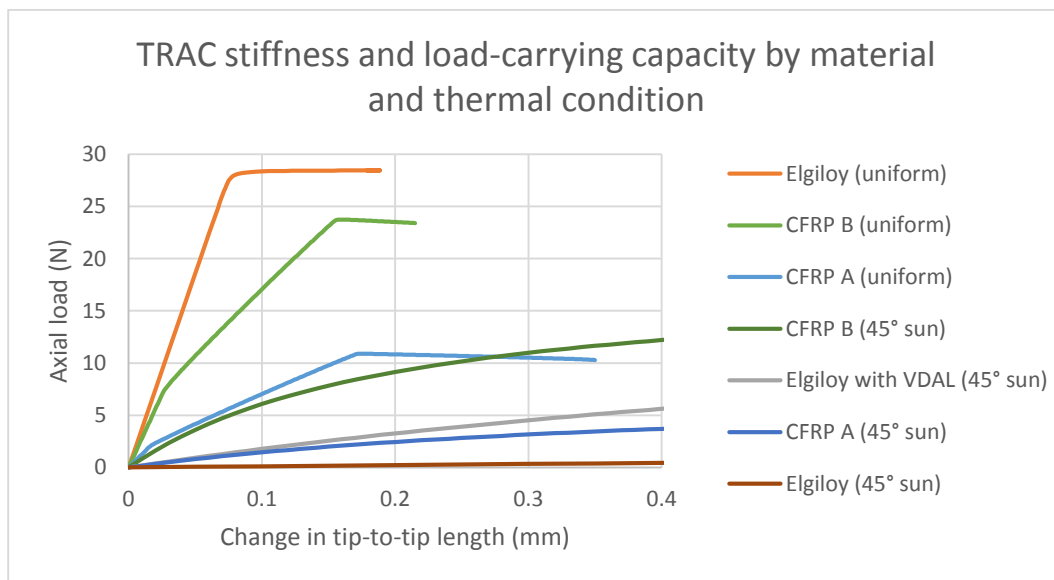

Figure 12: Changes in stiffness due to thermal distortion of booms.

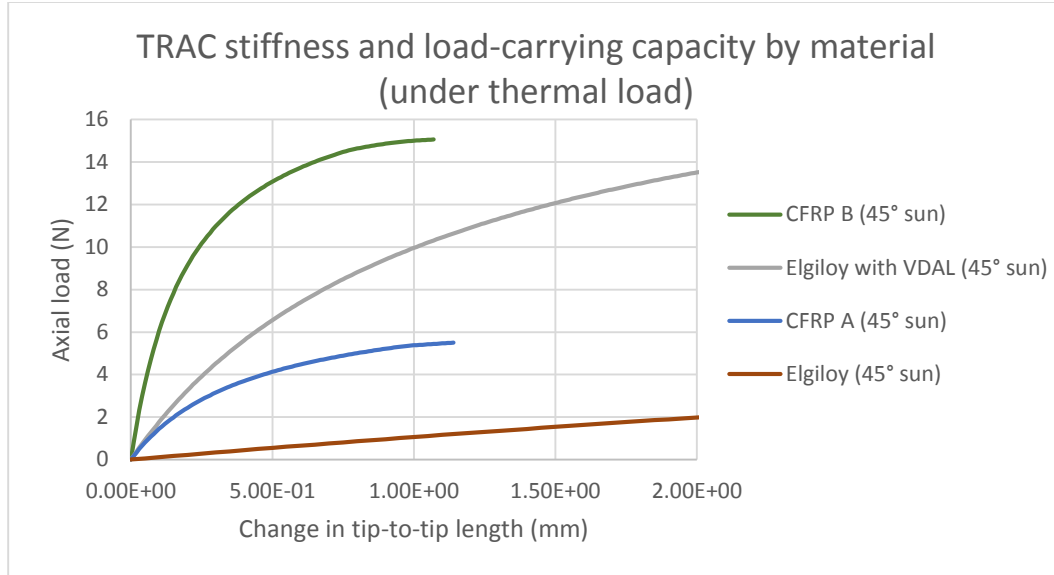American Institute of Aeronautics and Astronautics

Figure 13: Stiffness of thermally deformed booms by material.

Table 5: Structural performance changes due to thermal distortion. Stiffness is reported at zero load; booms lose stiffness in different patterns according to material properties.

	Stiffness (tip-to-tip compression) at uniform 298 K	Stiffness (tip-to-tip compression) at 45° sun angle
Elgiloy	373 N/m	1 N/m
Elgiloy with vapor-deposited aluminum coating	373 N/m	18 N/m
Carbon fiber composite A (thin)	126 N/m	14 N/m
Carbon fiber composite B (thick)	279 N/m	56 N/m

C. Structural Performance as Part of a Solar Sail

When the membranes are added to the structural model of the sail, the large-scale shape change induced by thermal gradients can be visualized, as in Figure 14. In the boom-and-membrane model, the sail membrane partially restricts the motion of the boom tips; this, in part, causes the booms to twist. This interaction does not prevent the booms from deforming, but does change the shape of the deformation. Twisting can be seen in Figure 15(b), which shows the boom-and-membrane model from the tip of a boom; twist is not present in the single-boom analysis of Figure 7. The results below for uncoated Elgiloy booms are path-dependent and not considered reliable on the centimeter level. This highlights the need for a coupled approach, like that presented by Blandino [12], if high-accuracy results are required.
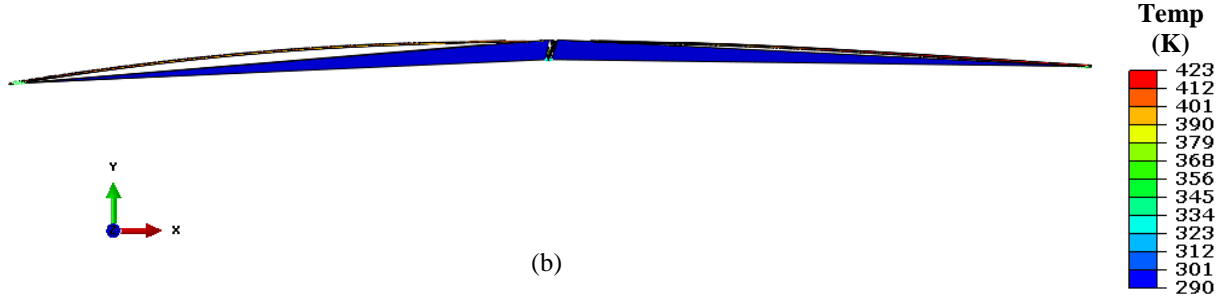

(a)

American Institute of Aeronautics and Astronautics
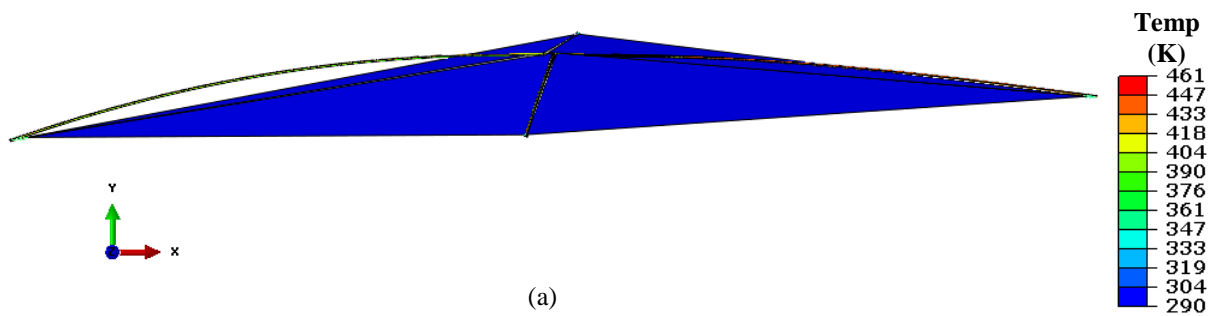
Figure 14: Uncoated (a) and VDAL-coated (b) sail systems. The sun side is +Y. The deformation scale factor is 1:1.
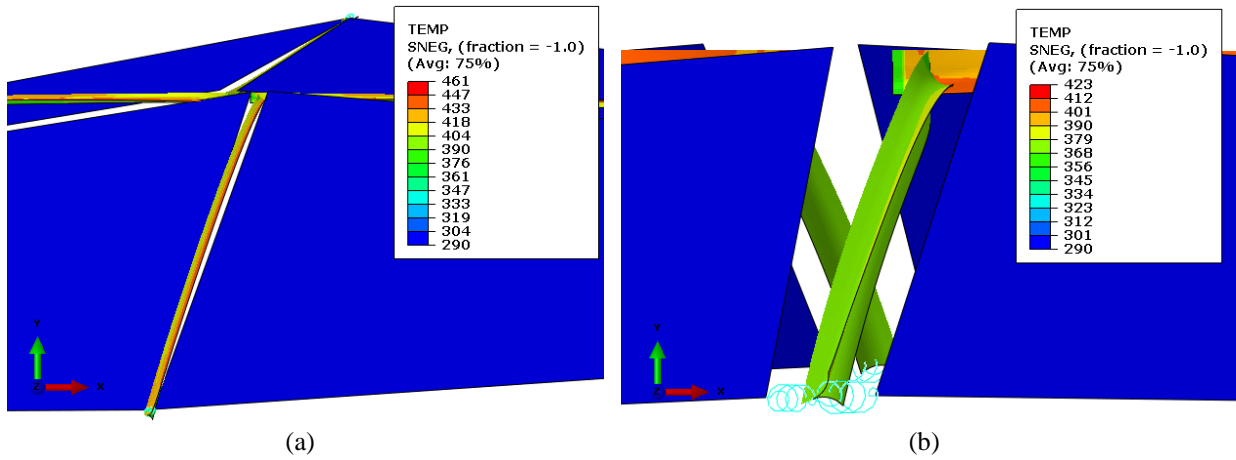

(a)   (b)

Figure 15: Close-up of booms from Figure 14: uncoated (a) and VDAL-coated (b). Note that the booms have twisted 90°, invalidating the original thermal solution. The deformation scale factor is 1:1.

IV.   The Planetary Society's LightSail-A

The Planetary Society operated the LightSail-A satellite from May 20th, 2015 to June 14th, 2015 [4], successfully testing deployment of a solar sail, and two pictures of the deployed sail (Figure 16) were downloaded during satellite operations. These are the only pictures taken in orbit of a rigid-boom-deployed solar sail, as NanoSail-D did not have a camera. It initially seemed possible that these images might contain enough data to distinguish a thermal deflection of the booms and validate the model; upon inspection, this is not possible with the existing data set. An explanation of that inspection is presented here in order to illustrate the small gap between the available data and what would be necessary to demonstrate thermal deformation and validate or refute the model.
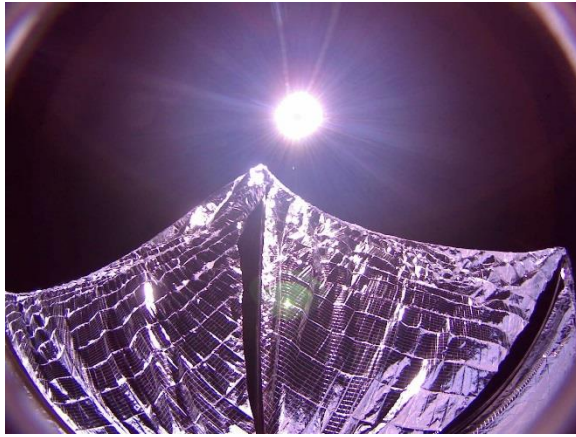
American Institute of Aeronautics and Astronautics

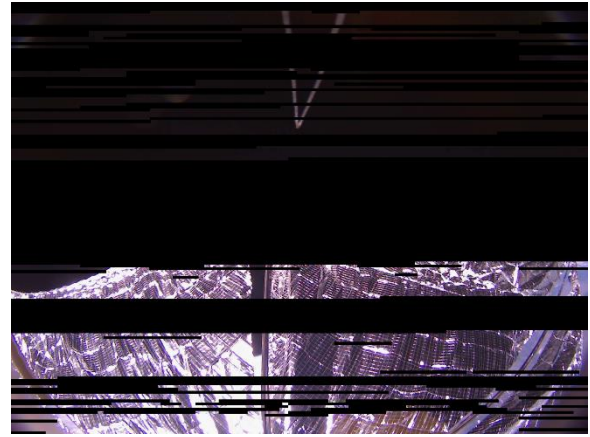Image: Planetary Society   Image: Emily Lakdawalla/Planetary Society [17]

(a)   (b)

Figure 16: The complete first (a) and incomplete second (b) downlinked images from LightSail-A. Note that the boom tips are not included in the second image, and that the sail edges are separated from the sail root by a band of absent data. Both pictures were taken from the same camera.

The sail membrane on LightSail-A was not pulled taut, so a very simple analysis of the boom distortions was done, without any modeling of the sail membrane itself or its structural effect on the booms. This analysis can only give a representative example of possible boom tip motion. Without knowing the precise sun angle at the moments of the photographs, as well as the satellite's recent attitude history, it is not possible to predict boom distortions for comparison with a specific image; further, there is an unpredictable shading effect from the rumpled sail membrane. Based on the approximate sun position in Figure 16(a), the sail was modeled as if one boom were pointed directly at the sun. This analysis produced the distorted boom shapes in Figure 17.
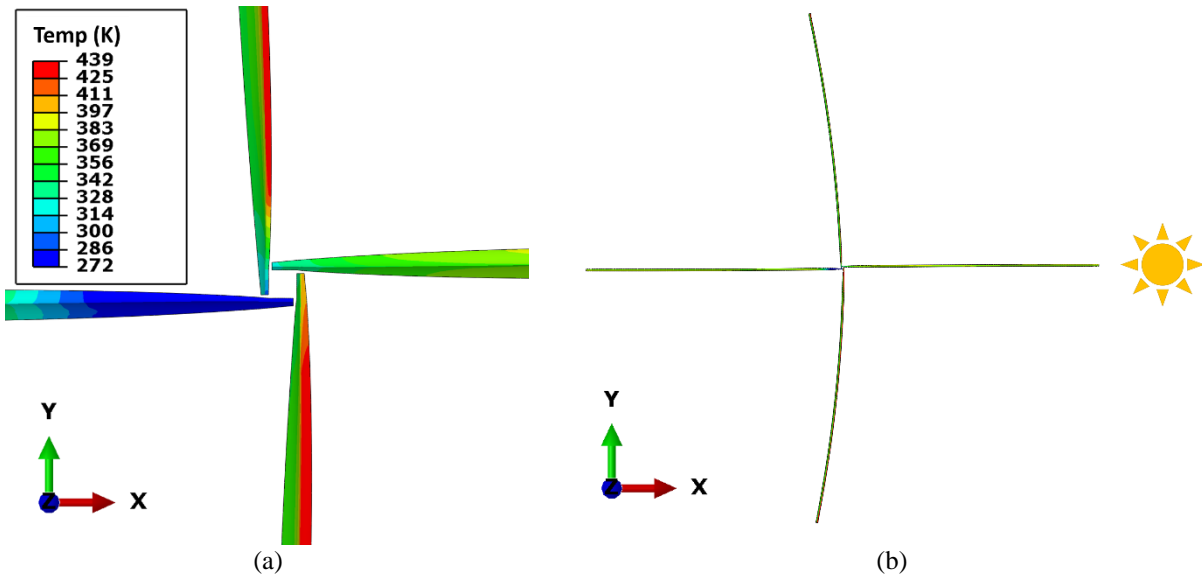

(a)   (b)

Figure 17: FEA simulation of Lightsail-length booms with sun at +X.

Using the lens projection function for LightSail-A's onboard cameras and an estimate of the Lightsail camera position, the images of thermally distorted booms were simulated (Figure 18). The cameras were optimized to capture the entire sail, rather than to study the boom tips in particular, but the motion of the boom tips could nonetheless be large enough to be distinguished if pictures were taken at the right combination of sun angles.
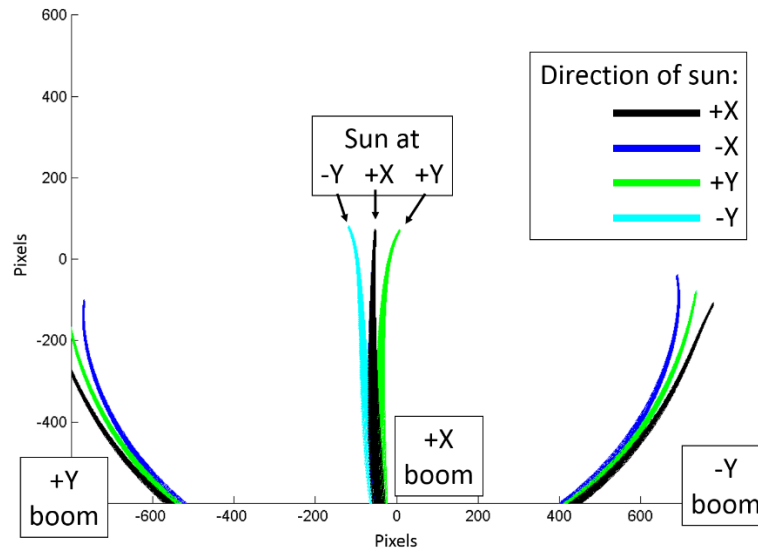
12

American Institute of Aeronautics and Astronautics

Figure 18: Simulated projection of thermally distorted LightSail-A booms. Sun is aligned with the X or Y axis of the spacecraft.

By coincidence, the partial second sail image does not include the boom tips. The satellite was also spinning at about 2.5 degrees/second [17]; this is too rapid for the Elgiloy booms to entirely reach steady-state at any sun orientation. For a sail edge-on to the sun, the range of boom tip motion from Figure 18 is overlaid on the LightSail-A images in Figure 19.
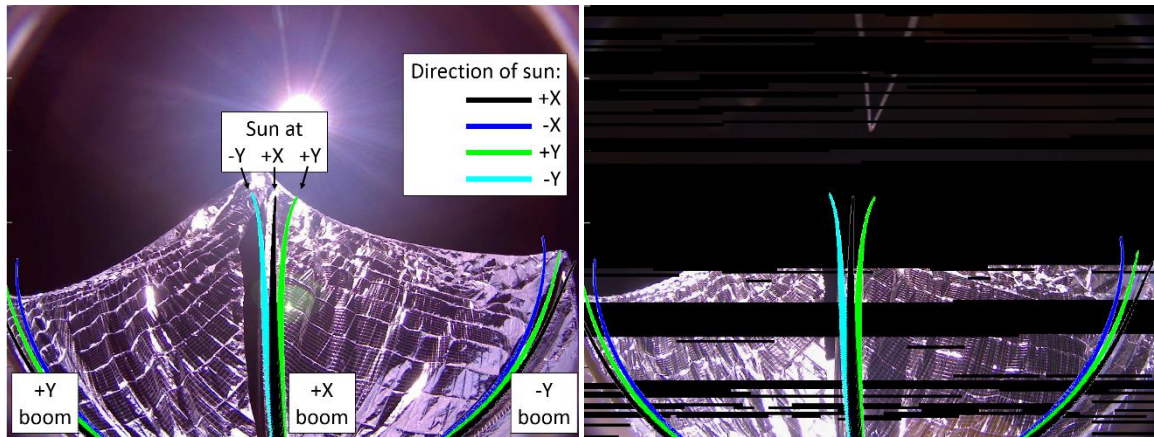

Figure 19: A range of possible boom distortions overlaid on the first (a) and second (b) sail images (composite of authors' data and Planetary Society images).

Because the attitude history of the spacecraft and the shading pattern of the sail membrane on the booms are uncertain, it is not possible to make a specific prediction of the deformed boom shapes for comparison against a single image, and validation of the model is not possible with the existing data. While it was possible that two pictures might have caught the booms at visibly different positions, the boom motion between these two images is very slight. It is difficult to draw any conclusion supporting or rejecting the presence of thermal deformation based on these results, but the authors hope that it provides some insight into the value of imaging to space structures analysis.

V.   Conclusions

Slender metallic booms are susceptible to extreme thermal distortion in the space environment. Distortions can be so large as to be visible in photographs of ordinary resolution.

Material alternatives were considered in this paper, and some crucial trends were identified, namely:

American Institute of Aeronautics and Astronautics

- A low-emissivity, low-absorptivity coating, vapor-deposited aluminum, is shown to reduce the thermally induced curvature from the uncoated Elgiloy case at the worst-case sun angle by a factor of four
- An uncoated carbon fiber composite, despite developing an extreme temperature gradient, experiences less induced curvature at the worst-case sun angle than uncoated Elgiloy by a factor of ten
- Despite having a lower material stiffness, booms made of carbon fiber outperformed uncoated Elgiloy booms in compressive stiffness at a worst-case sun angle, because of their lower curvature
- Carbon fiber composites are competitive with coated Elgiloy where there is enough volume margin to accept a somewhat thicker boom material

In comparing material alternatives, the thermally deformed case should be considered early in the structural design. The elastic modulus of the boom material was not, in the cases examined here, decisive in the stiffness of the booms as a whole. Rather, boom stiffness was dominated by the induced radius of curvature. The ideal material and coating would have a low coefficient of axial thermal expansion, high transverse thermal conductivity, low solar absorptivity, and low thermal emissivity.

Other design alternatives are also effective. First among these is shading the boom- the same strategy that is preferred for high-precision or cryogenic structures. Booms with a substantial component of axially aligned unidirectional carbon fiber can have a very low axial coefficient of thermal expansion. In many cases, it is possible to avoid severe thermal distortion by avoiding monolithic tape-spring booms altogether. Booms with a sparse truss structure, for example, avoid dramatic shading effects at most angles.

Finally, LightSail-A came tantalizingly close to demonstrating thermal deformation of ultra-slender booms- a small number of downlinked images, of modest resolution, could show this effect, much as the increased stiffness of a crinkled membrane was demonstrated by IKAROS images [18]. Ideally, a higher-accuracy model of the LightSail booms and membrane could be combined with a larger number of images and more precise knowledge of the attitude history for model validation. The Planetary Society's LightSail-B, expected to launch in 2016 [19], may provide us with the best experimental data on this space environment effect to date.

Acknowledgments

References

[1]   J. Banik and T. Murphey, "Triangular rollable and collapsible boom". United States Patent 7,895,795, 2011.

[2]   J. A. Banik and T. W. Murphey, "Peformance validation of the triangular rollable and collapsible mast," in *24th Annual AIAA/USU Conference on Small Satellites*, Logan, UT, 2010.

[3]   L. Johnson, M. Whorton, A. Heaton, R. Pinson, G. Laue and C. Adams, "NanoSail-D: A solar sail demonstration mission," *Acta Astronautica,* vol. 68, no. 5-6, pp. 571-575, 2011.

[4]   The Planetary Society, "LightSail," 2015. [Online]. Available: http://sail.planetary.org/. [Accessed May 2015].

[5]   L. McNutt, L. Johnson, D. Clardy, J. Castillo-Rogez, A. Frick and L. Jones, "Near-Earth Asteroid Scout," in *AIAA Space Conference*, San Diego, CA, 4-7 August 2014.

[6]   B. Cohen, P. Hayne, B. Greenhagen and D. Paige, "Lunar Flashlight: mapping lunar surface volatiles using a Cubesat (presentation)," in *Annual Meeting of the Lunar Exploration Analysis Group*, 2013.

[7]   C. Biddy and T. Svitek, "LightSail-1 solar sail design and qualification," in *41st Aerospace Mechanisms Symposium*, Jet Propulsion Laboratory, 16-18 May 2012.

[8]   M. Hillebrandt, S. Meyer, M. Zander and C. Huhne, "Deployment testing of the De-Orbit Sail flight hardware," in *2nd AIAA Spacecraft Structures Conference*, Kissimmee, FL, 5-9 January 2015.

[9]   J. M. Fernandez, L. Visagie, M. Schenk, O. R. Stohlman, G. S. Aglietti, V. J. Lappas and S. Erb, "Design and development of a gossamer sail system for deorbiting in low earth orbit," *Acta Astronautica,* vol. 103, pp. 204-225, 2014.

[10] C. Sickinger, L. Herbeck and E. Breitbach, "Structural engineering on deployable CFRP booms for a solar propelled sailcraft," *Acta Astronautica,* vol. 58, pp. 185-196, 2006.

American Institute of Aeronautics and Astronautics

[11] Clyde Space, "AEOLDOS, De-orbit devices CubeSat," 2015. [Online]. Available: http://www.clyde-space.com/cubesat_shop/de-orbit_devices/349_aeoldos. [Accessed May 2015].

[12] J. R. Blandino, "Analysis of thermal-mechanical interactions of STEM booms," in *2nd AIAA Spacecraft Structures Conference*, Kissimmee, FL, 5-9 January 2015.

[13] M. E. McEachen, "Development of the GEMS telescope optical boom," in *52nd AIAA/ASME/ASCE/AHS/ASC SDM Conference*, Denver, CO, 4-7 April 2011.

[14] D. Gilmore, Spacecraft thermal control handbook, El Segundo, CA: Aerospace Press, 2002.

[15] L. Kauder, "Spacecraft thermal control coatings reference," NASA/Goddard Space Flight Center, Greenbelt, MD, 2005.

[16] Dassault Systemes, Abaqus 6.11 documentation, 2011.

[17] J. Davis, "Pretty (partial) picture: LightSail catches a glimpse of Earth," Planetary Society, 11 6 2015. [Online]. Available: http://www.planetary.org/blogs/jason-davis/2015/20150610-lightsail-cathes-glimpse-earth.html. [Accessed 11 11 2015].

[18] Y. Shirasawa, O. Mori, N. Okuizumi, Y. Satou, A. Yamasaki, H. Furuya, T. Mishizawa, H. Sakamoto and G. Ono, "Evaluation of sail mechanics of IKAROS on its slow-spin and reverse-spin operation," in *Advances in Solar Sailing*, Springer Berlin Heidelberg, 2014, pp. 54-74.

[19] R. Ridenoure, R. Munakata, A. Diaz, S. Wong, B. Plante, D. Stetson, D. Spencer and J. Foley, "LightSail program status: one down, one to go," in *29th Annual AIAA/USU Conference on Small Satellites*, Logan, UT, 2015.

American Institute of Aeronautics and Astronautics